Multiple roles for the C-terminal domain of eIF5 in translation initiation complex assembly and GTPase activation

Katsura Asano[1], Anath Shalev, Lon Phan, Klaus Nielsen, Jason Clayton, Leoš Valášek, Thomas F.Donahue[2] and Alan G.Hinnebusch[3]

Laboratory of Gene Regulation and Development, National Institute of Child Health and Human Development, NIH, Bethesda, MD 20892 and [2]Department of Biology, Indiana University, Bloomington, IN 47405, USA

[1]Present address: Division of Biology, Kansas State University, Manhattan, KS 66506, USA

[3]Corresponding author
e-mail: ahinnebusch@nih.gov

eIF5 stimulates the GTPase activity of eIF2 bound to Met-tRNA$_i^{Met}$, and its C-terminal domain (eIF5-CTD) bridges interaction between eIF2 and eIF3/eIF1 in a multifactor complex containing Met-tRNA$_i^{Met}$. The *tif5-7A* mutation in eIF5-CTD, which destabilizes the multifactor complex *in vivo*, reduced the binding of Met-tRNA$_i^{Met}$ and mRNA to 40S subunits *in vitro*. Interestingly, eIF5-CTD bound simultaneously to the eIF4G subunit of the cap-binding complex and the NIP1 subunit of eIF3. These interactions may enhance association of eIF4G with eIF3 to promote mRNA binding to the ribosome. *In vivo*, *tif5-7A* eliminated eIF5 as a stable component of the pre-initiation complex and led to accumulation of 48S complexes containing eIF2; thus, conversion of 48S to 80S complexes is the rate-limiting defect in this mutant. We propose that eIF5-CTD stimulates binding of Met-tRNA$_i^{Met}$ and mRNA to 40S subunits through interactions with eIF2, eIF3 and eIF4G; however, its most important function is to anchor eIF5 to other components of the 48S complex in a manner required to couple GTP hydrolysis to AUG recognition during the scanning phase of initiation.
Keywords: eukaryotic translation initiation factor (eIF)/ GAP/Met-tRNA$_i^{Met}$ binding/mRNA binding/scanning

Introduction

The selection of initiation codons in mRNAs during the initiation of protein synthesis is a highly regulated process in eukaryotic cells, involving the 40S ribosomal subunit and numerous eukaryotic initiation factors (eIFs). The 40S ribosome binds to the eIF2–GTP–methionyl initiator tRNA (Met-tRNA$_i^{Met}$) ternary complex (TC) to form the 43S pre-initiation complex. Subsequent joining of the mRNA in association with eIF4F bound to the m^{7}G cap produces the 48S pre-initiation complex. eIF3 stimulates recruitment of Met-tRNA$_i^{Met}$ and mRNA to the 40S ribosome (for a review see Hershey and Merrick, 2000). Formation of a 48S complex positioned at the AUG start codon is dependent on eIF1, eIF1A, eIF4A and eIF4B, in

addition to eIF2, eIF3 and eIF4F (Pestova *et al.*, 1998). In current models, eIF5 binds to a positioned 48S complex and stimulates GTP hydrolysis by eIF2, acting as a GTPase-activating protein (GAP), prior to ejection of all eIFs and joining of the 60S subunit (Chakrabarti and Maitra, 1991; Huang *et al.*, 1997). In the yeast *Saccharomyces cerevisiae*, *SUI* (suppressor of initiation codon) mutations were isolated in eIF1, eIF5 and all three subunits of eIF2, which allow ribosomes to select UUG as the start codon at elevated frequencies (for a review see Donahue, 2000). Biochemical analysis suggests that a higher rate of GTP hydrolysis on eIF2 is responsible for the reduced accuracy of AUG selection in the Sui$^-$ mutants (Huang *et al.*, 1997). Thus, accurate initiation requires tight coupling between the GAP activity of eIF5 and base pairing between Met-tRNA$_i^{Met}$ and the start codon.

eIF1 and the C-terminal domain of eIF5 (eIF5-CTD) both bind to the eIF3 subunit NIP1 (Asano *et al.*, 1998, 2000; Phan *et al.*, 1998), suggesting that the functions of eIF1 and eIF5 in AUG recognition are coordinated by eIF3. Additionally, eIF5-CTD can bind to the β-subunit of its substrate eIF2 (Asano *et al.*, 1999). A bipartite sequence motif of aromatic and acidic amino acids (AA-boxes) in eIF5-CTD is required for its interaction with eIF3-NIP1 and eIF2β (Asano *et al.*, 1999; Das and Maitra, 2000), and the latter interaction is dependent on lysine-rich stretches (K-boxes) in the N-terminal half of eIF2β (Das *et al.*, 1997; Asano *et al.*, 1999). Alanine substitutions altering all 12 conserved residues in AA-box 1 (*tif5-12A*) or all seven residues in AA-box 2 (*tif5-7A*) of eIF5-CTD disrupted its interactions with eIF3-NIP1 and eIF2β *in vitro*. These mutations are lethal (*tif5-12A*) or confer temperature sensitivity (Ts$^-$) and slow growth (Slg$^-$) (*tif5-7A*) in yeast cells. At a semi-permissive temperature, *tif5-7A* disrupted interaction between eIF5 and native eIF2 and eIF3 complexes *in vivo* (Asano *et al.*, 1999).

The interactions of eIF3-NIP1 with eIF1 and eIF5-CTD, and of eIF5-CTD with eIF3-NIP1 and eIF2β, occur simultaneously *in vitro*, suggesting that these eIFs reside in the same multifactor complexes (MFCs). We observed such complexes containing eIFs 1, 2, 3 and 5 and stoichiometric amounts of tRNA$_i^{Met}$ in cell extracts, and showed that they were destabilized by the *tif5-7A* mutation in eIF5-CTD or by K-box mutations in eIF2β. As *tif5-7A* reduced the polyribosome content in yeast cells, it appears that the MFC is an important intermediate in translation initiation *in vivo* (Asano *et al.*, 2000). The MFC could be purified free of ribosomes, suggesting that its constituent factors bind to 40S subunits as a pre-formed unit and remain associated in the 48S initiation complex during the scanning process. If so, the functions of eIFs 1, 2, 3 and 5 in recruitment of Met-tRNA$_i^{Met}$ and mRNA to the ribosome,
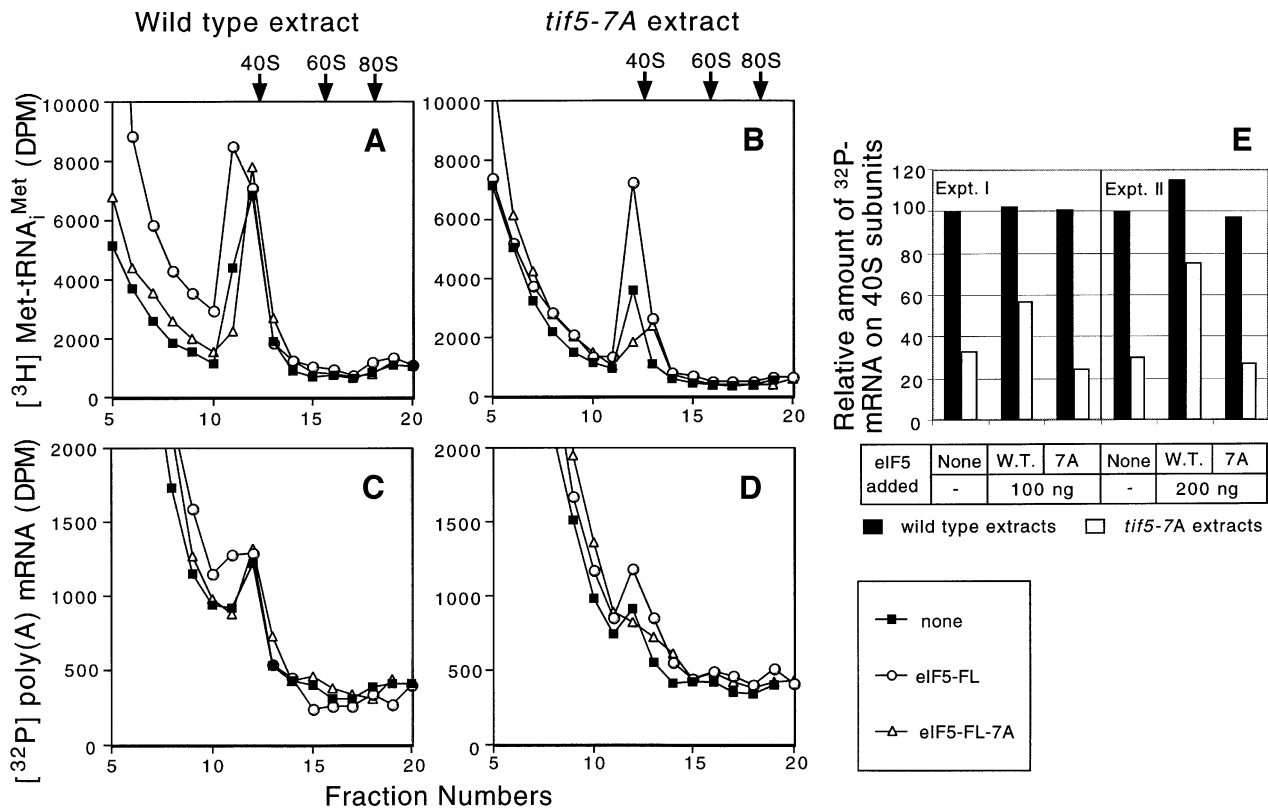
Fig. 1. *tif5-7A* impairs the binding of Met-tRNA$_i^{Met}$ and poly(A) mRNA to 40S ribosomes *in vitro*. Translation-competent extracts were prepared from KAY35 (*TIF5*) and KAY36 (*tif5-7A*) (Asano *et al.*, 1999) and measured for the ability to transfer exogenous [^{3}H]Met-tRNA$_i^{Met}$ (**A** and **B**) and [^{32}P]poly(A) *MFA2* mRNA (**C** and **D**) to 40S ribosomes in the presence of 1.2 mM GMPPNP. Some of the reactions also contained 0.2 μg of purified native eIF5-FL or eIF5-FL-7A. The reactions were resolved by sucrose gradient–velocity sedimentation and the amounts of [^{3}H]Met-tRNA$_i^{Met}$ and [^{32}P]poly(A) mRNA in each reaction were determined by scintillation counting. Arrows indicate the positions of 40S, 60S and 80S ribosomes, determined from the A_{254} profiles of the gradients. The data shown are typical results of several independent experiments. (**E**) The data from two independent experiments of the type described in (C) and (D) were quantified by summing the radioactivity in fractions 11–13 and subtracting the baseline values obtained with wild-type or mutant extracts to which [^{32}P]poly(A) mRNA, but no eIF5, was added and the incubation at 26°C was omitted.

and in AUG recognition, might all depend on the integrity of the MFC.

In this study, we investigated which reactions in the initiation pathway are impaired when the MFC is disrupted by the *tif5-7A* mutation in eIF5-CTD. Consistent with the fact that eIF5-CTD bridges interaction between eIF2 and eIF3, and the known function of eIF3 in TC binding, we found that *tif5-7A* decreases the rate of Met-tRNA$_i^{Met}$ binding to 40S subunits *in vitro*. Interestingly, mRNA binding to 40S ribosomes was also compromised by this mutation. Pursuing the latter finding, we discovered that eIF5-CTD interacts with the C-terminal half of eIF4G, the largest subunit of eIF4F (Hentze, 1997; Sachs *et al.*, 1997), and bridges interaction between eIF3 and eIF4G both *in vivo* and *in vitro*.

In vivo, we found that *tif5-7A* greatly reduced the association of eIF5 with native 43–48S complexes. Moreover, 48S complexes containing all other components of the MFC accumulated in the *tif5-7A* mutant, indicating a block late in the pathway where eIF5 GAP function is required. Thus, while eIF5-CTD promotes Met-tRNA$_i^{Met}$ and mRNA binding to 40S subunits *in vitro*, its rate-limiting function *in vivo* is the stable incorporation of eIF5 into pre-initiation complexes in a manner required for coupling GTP hydrolysis to AUG recognition.

Results

tif5-7A impairs binding of Met-tRNA$_i^{Met}$ and poly(A) mRNA to 40S ribosomes *in vitro*

Given the function of eIF3 in stimulating TC binding to 40S ribosomes (Hinnebusch, 2000) and the role of eIF5-CTD in bridging interaction between eIF3 and eIF2 in the MFC (Asano *et al.*, 2000), we hypothesized that eIF5-CTD would promote TC binding to 40S ribosomes. To test this idea, we prepared extracts from isogenic wild-type and *tif5-7A* mutants and assayed the transfer of exogenous [^{3}H]Met-tRNA$_i^{Met}$ to 40S ribosomes in the presence of a non-hydrolyzable GTP analog (GMPPNP). The latter was included to prevent hydrolysis of GTP in the TC and subsequent joining of 60S subunits to 48S initiation complexes (Phan *et al.*, 1998). As shown in Figure 1A and B (filled squares), much less [^{3}H]Met-tRNA$_i^{Met}$ bound to 40S ribosomes in the *tif5-7A* extract compared with the wild-type extract. Importantly, this defect was complemented by addition of purified FLAG epitope-tagged eIF5 (eIF5-FL; open circles) but not by the *tif5-7A* mutant version of this protein (eIF5-FL-7A; open triangles). Thus, *tif5-7A* decreased the binding of Met-tRNA$_i^{Met}$ to 40S ribosomes in cell extracts.

We also examined the effect of *tif5-7A* on mRNA binding to 40S ribosomes in the same extracts using exogenous [^{32}P]*MFA2* polyadenylated mRNA (Tarun and Sachs, 1995), again in the presence of GMPPNP. Interestingly, [^{32}P]*MFA2* mRNA binding was reduced significantly in the *tif5-7A* extract (Figure 1C and D, filled squares), and this defect was complemented by purified wild-type eIF5-FL (open circles) but not by eIF5-FL-7A (open triangles). The defect in mRNA binding could be a secondary consequence of reduced Met-tRNA$_i^{Met}$ binding in the *tif5-7A* extract (Hinnebusch, 2000). Alternatively, it may signify a role for eIF5-CTD in mRNA recruitment to the 40S ribosome during 48S complex assembly.

tif5-7A reduces interaction between eIF3 and eIF4G in vivo

In view of the evidence that mRNA is recruited to the 40S ribosome through interaction between eIF3 and eIF4G (Sachs *et al.*, 1997), and the fact that eIF5 is stably associated with eIF3, we considered the possibility that eIF5-CTD contributes to association between eIF4G and eIF3. If so, the mRNA binding defect conferred by *tif5-7A* could arise at least partly from destabilization of an eIF3–eIF5–eIF4G complex. Previously, we detected association of a small fraction of eIF4G with eIF3 in yeast cell extracts (Phan *et al.*, 1998). To determine whether *tif5-7A* reduces this interaction, we immunoprecipitated eIF3 using anti-hemagglutinin (HA) antibodies directed against an HA epitope-tagged version of eIF3 subunit TIF34. As expected, the majority of eIF3 subunit PRT1 co-immuno-precipitated with HA-TIF34 from both *TIF5* and *tif5-7A* extracts (Figure 2, lanes 1–6), whereas no PRT1 was immunoprecipitated from an extract containing untagged TIF34 (lanes 7–9). Probing the immune complexes with antibodies against eIF5, eIF1 and eIF2α confirmed that *tif5-7A* disrupted association between eIF2 and eIF3/eIF1 *in vivo* (Asano *et al.*, 2000). Probing the same complexes for eIF4G1, one of the two isoforms of yeast eIF4G, we found that ~3% of eIF4G1 specifically co-immunopre-cipitated with HA-TIF34 (Figure 2, lanes 2 and 8), and this interaction was reduced by *tif5-7A* (lanes 2 and 5). Thus, it is possible that eIF5-CTD enhances interaction between eIF3 and eIF4G. None of the m^{7}G cap-binding subunit of eIF4F, eIF4E, was co-immunoprecipitated with HA-TIF34 (Figure 2, lane 2), suggesting that yeast eIF4F complexes associated with eIF3 are relatively unstable.

eIF5-CTD binds directly to the C-terminal half of eIF4G2 in vitro

The results described above raised the possibility that eIF5-CTD binds directly to eIF4G to stabilize eIF3–eIF4G association. Accordingly, we tested purified eIF5-FL for binding to glutathione *S*-transferase (GST) fusions made to full-length eIF4G1 or eIF4G2. Both fusions bound specifically to wild-type eIF5-FL (Figure 3A, lanes 4–7) and this interaction was reduced to ~30–50% by the *tif5-7A* mutation (lanes 8–11). In contrast, the GST–eIF4G proteins did not bind to purified eIF2 (lanes 12–15). The interactions of eIF5 with the GST–eIF4G proteins were resistant to treatment with RNases (data not shown and see Materials and methods), supporting a direct interaction between these proteins.
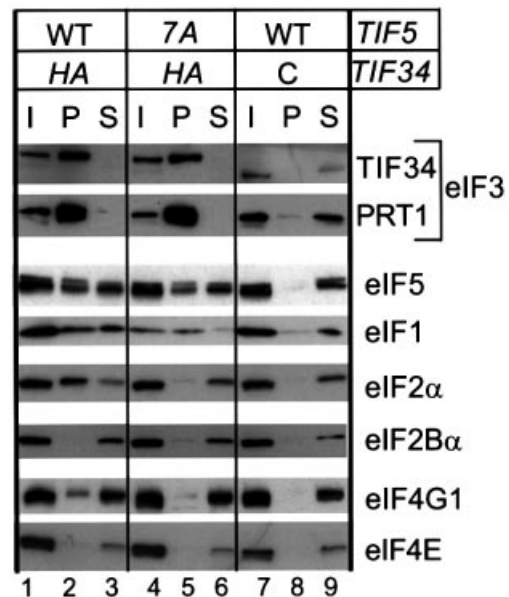

Fig. 2. The eIF5-CTD mediates interaction of eIF3 with eIF2 and eIF4G *in vivo*. Whole-cell extracts (WCEs) were prepared from strains KAY50 (*TIF34-HA TIF5-FL*) (lanes 1–3), KAY51 (*TIF34-HA tif5-FL-7A*) (lanes 4–6) and KAY37 (*TIF34 TIF5-FL*) (lanes 7–9) (Asano *et al.*, 2000) grown in YPD medium at 30°C. Aliquots of WCEs were incubated with anti-HA affinity resin and, after extensive washing, the bound proteins were analyzed by SDS–PAGE and immunoblotting with antibodies against the proteins indicated on the right. Lanes 1, 4 and 7, 20% input (I) amounts of WCE; lanes 2, 5 and 8, the entire precipitated (P) fractions; lanes 3, 6 and 9, 10% of supernatant (S) fractions. The top panel describes the presence of wild-type (WT) or *tif5-7A* (7A) forms of eIF5 in the extracts, and the presence (HA) or absence (C) of the HA-epitope on eIF3-TIF34.

To localize the interaction, we synthesized the two halves of eIF4G2 in rabbit reticulocyte lysates, labeling them with [^{35}S]methionine, and tested the labeled poly-peptides for binding to GST fusions containing full-length or truncated forms of eIF5. The eIF4G2 C-terminal fragment (eIF4G2-C), but not the N-terminal fragment (eIF4G2-N), bound specifically to GST–eIF5 (Figure 3B, lanes 5 and 8). The proportion of eIF4G2-C that bound to GST–eIF5 (~5%) was lower than the 30–50% binding of eIF3-NIP1 or eIF2β to GST–eIF5 that we observed under similar conditions (Asano *et al.*, 1999). Thus, the eIF5–eIF4G2 interaction is weaker than the eIF5–eIF2 or eIF5–eIF3 interactions described previously.

We then investigated whether eIF5-CTD mediates the interaction of eIF5 with the C-terminal half of eIF4G. Introducing the *tif5-12A* and *tif5-7A* mutations into the AA-boxes of GST–eIF5 reduced, but did not abolish, its interaction with the [^{35}S]eIF4G2-C fragment (Figure 4A, lanes 3–5). Similar results were obtained for C-terminal deletions removing the AA-boxes from GST–eIF5 in constructs A8 and A9 (Figure 4A and B, lanes 12–14). In contrast, deletions that removed only the N-terminal half of eIF5 from the GST–eIF5 fusion (in constructs B5 and B6) enhanced the interaction with [^{35}S]eIF4G2-C, whereas larger deletions from the N-terminus that additionally removed residues from the CTD (in constructs B7 and B8) abolished this high-level binding (Figure 4, lanes 3 and 6–9). Thus, the CTD is necessary and sufficient for interaction of GST–eIF5 with the C-terminal half of eIF4G2. Finally, introducing the *tif5-12A* and *tif5-7A*
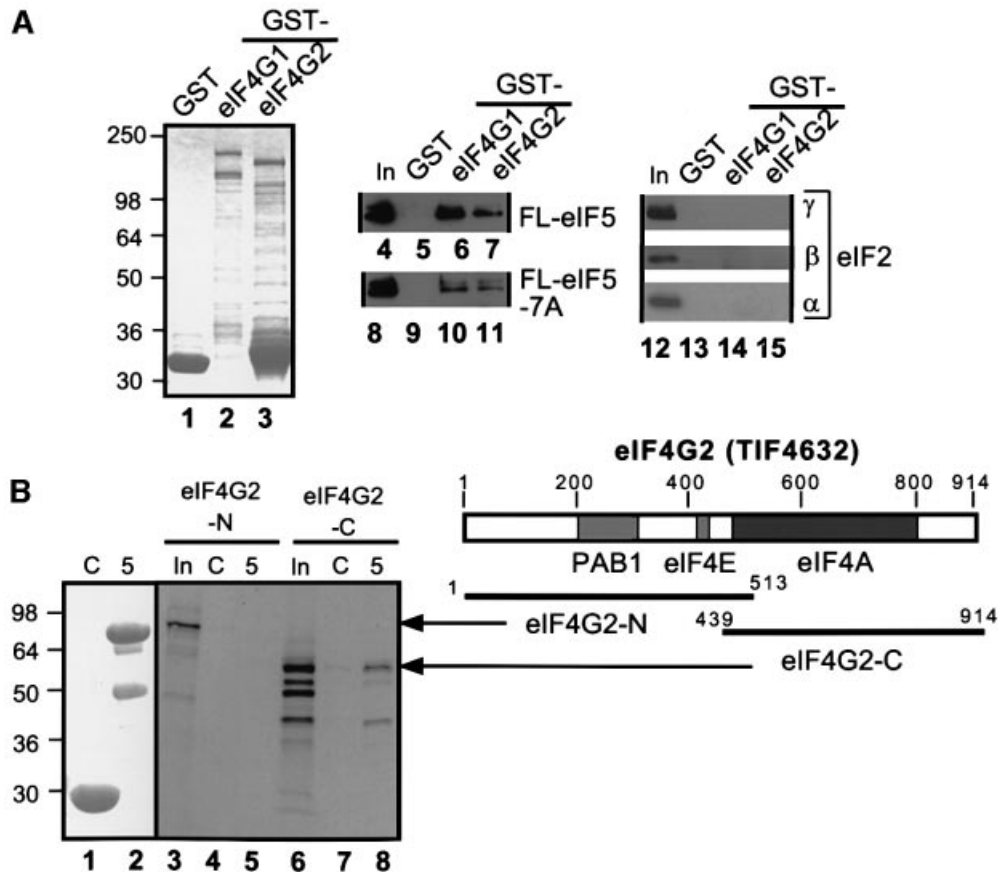
Fig. 3. eIF5 interacts with eIF4G *in vitro*. (**A**) Binding of GST–eIF4G to native eIF2 or recombinant eIF5-FL. Lanes 1–3, Coomassie Blue staining following SDS–PAGE of GST, GST–eIF4G1 and GST–eIF4G2 proteins used in the assays. Aliquots containing ~5 μg of GST or ~1 μg of the full-length GST–eIF4G fusion proteins were incubated with 100 ng of either recombinant eIF5-FL (lanes 4–7) or eIF5-FL-7A (lanes 8–11), or 1 μg of eIF2 (lanes 12–15). Proteins bound to the GST fusions were isolated with glutathione–Sepharose beads (GST pull-down) and analyzed by immunoblotting with the appropriate polyclonal antibodies, except that anti-FLAG antibodies were used for detecting eIF5-FL and eIF5-FL-7A. Lanes 4, 8, 12 and 16, 20% of input (In) amount of the indicated proteins. (**B**) Binding of GST–eIF5 to segments of eIF4G2 in GST pull-down assays. Aliquots containing ~5 μg of GST (C) or GST–eIF5 (5), shown in a Coomassie Blue-stained gel following SDS–PAGE in lanes 1 and 2, were incubated with [^{35}S]eIF4G2-N (lanes 3–5) or eIF4G2-C (lanes 6–8), and the bound proteins were separated by SDS–PAGE, followed by autoradiography and phosphoimaging analyses. In, 50% input amount. The amino acids present in the eIF4G2 segments are indicated on the bars shown beneath the box depicting the primary structure of yeast eIF4G2. Gray boxes in the latter denote the binding sites for the indicated proteins (Tarun and Sachs, 1996; Neff and Sachs, 1999).

mutations into the GST–eIF5-B6 construct containing only the CTD greatly reduced its binding to [^{35}S]eIF4G2-C (Figure 4A, lanes 16–18), confirming that the AA-boxes are important constituents of the eIF4G-binding domain in eIF5-CTD. The increased binding activity of the N-terminally truncated constructs B5 and B6 versus full-length GST–eIF5 might indicate that the N-terminus of eIF5 interferes with the ability of the CTD to interact with eIF4G2-C.

eIF5-CTD can bridge interactions between eIF3-NIP1 and eIF4G in vitro

If eIF5-CTD promotes eIF4G–eIF3 interaction, we would predict that eIF5-CTD can interact simultaneously with eIF4G2-C and the N-terminus of eIF3-NIP1. In addition to testing this prediction, we wished to determine whether the eIF4G–eIF5-CTD interaction is compatible with stable association between eIF5-CTD and the K-box domain of eIF2β (Figure 5A). To address these questions, we purified polyhistidine-tagged N-terminal segments of NIP1 and eIF2β (His-NIP1N and His-eIF2β-N, respectively) con-

taining the binding domains in these proteins for eIF5-CTD (Asano *et al.*, 1999, 2000) and tested them for effects on the interaction between [^{35}S]eIF4G2-C and GST–eIF5-B6 (containing the CTD). We found that GST–eIF5-B6 bound efficiently to [^{35}S]eIF4G2-C when His-NIP1-N was present at a 25-fold molar excess over GST–eIF5-B6 (Figure 5B, bottom panel, lanes 1–5). As expected, a fraction of His-NIP1-N itself bound to GST–eIF5-B6 in this experiment (Figure 5B, top panel, lanes 3–5), confirming the ability of these two recombinant proteins to interact directly. These findings suggest that the eIF4G2–eIF5 interaction does not compete with NIP1–eIF5 association *in vitro*.

In sharp contrast to the findings above, [^{35}S]eIF4G2-C did not bind to GST–eIF5-B6 in the presence of His-eIF2β-N added to the reaction (Figure 5C, bottom panel, lanes 6–10). (The lowest amount of His-eIF2β-N examined in lane 8 is equimolar to the amount of GST–eIF5-B6 and should be sufficient to reduce interaction between GST–eIF5-B6 and [^{35}S]eIF4G2-C by competition.) A portion of His-eIF2β-N was found
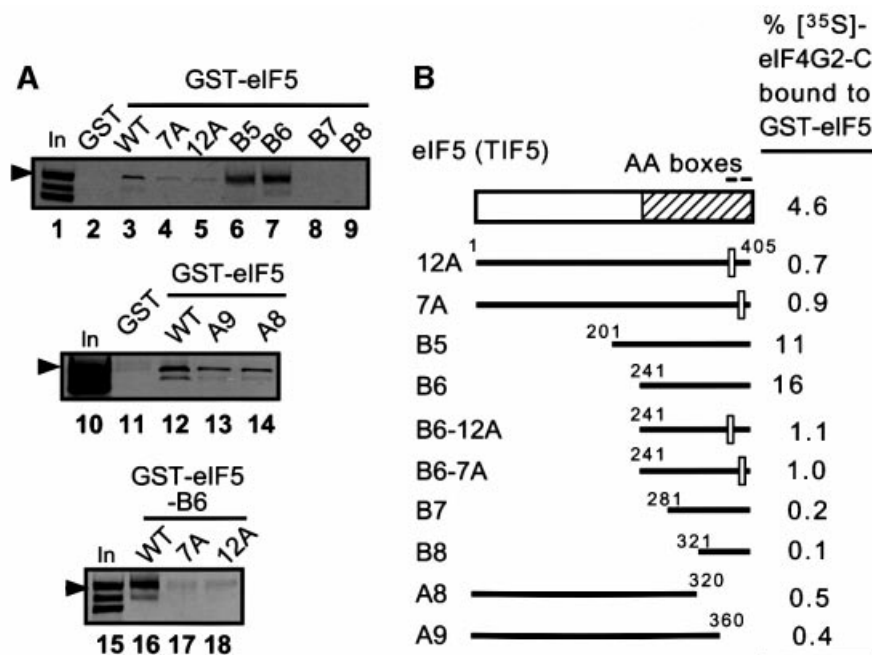
Fig. 4. AA-boxes in eIF5-CTD mediate its binding to eIF4G2. (**A**) Binding of GST–eIF5 derivatives to eIF4G2-C. GST, GST–eIF5 and its derivatives described in (B) were tested for binding to [^{35}S]eIF4G2-C, as in Figure 3B. In, 50% input amount. Arrowheads indicate full-length eIF4G2-C. (**B**) Summary of *in vitro* interactions between GST–eIF5 and [^{35}S]eIF4G2-C. The box at the top indicates the primary structure of yeast eIF5, with the minimal binding domains for eIFs 2, 3 and 4G shown by a hatched box. Bars beneath it represent the eIF5 segments used as GST fusions for *in vitro* binding assays in (A), with their designations shown to the left. Empty squares on the bars represent 12 and 7 alanine substitutions for AA-boxes 1 and 2 in *tif5-12A* and *tif5-7A*, respectively (Asano *et al.*, 1999).

associated with GST–eIF5-B6 (Figure 5C, top panel), confirming the ability of these two proteins to form a complex. These results suggest that the eIF4G–eIF5 interaction is mutually exclusive with the eIF2β–eIF5 interaction.

To confirm our conclusion that eIF5-CTD can bind simultaneously to eIF4G2 and eIF3-NIP1, we investigated whether the eIF5-B6 segment can bridge an interaction between [^{35}S]eIF4G2-C and a GST fusion containing the N-terminal domain of NIP1 (GST–NIP1-N). Supporting this idea, we found that [^{35}S]eIF4G2-C and GST–NIP1-N did not interact with one another unless the eIF5-B6 fragment was present in the reaction, being added in 25-fold molar excess to GST–NIP1-N (Figure 5E). Thus, eIF5-CTD can bridge interactions between eIF3 and either eIF2 or eIF4F through simultaneous binding to NIP1 and either eIF2β or eIF4G, respectively. In contrast, eIF5-CTD can not bridge interaction between eIF2 and eIF4F because its binding to eIF2β and eIF4G is mutually exclusive (Figure 5A). Below, we present a possible rationale for the ability of the eIF5-CTD–NIP1-N binary complex to form mutually exclusive ternary interactions with eIF4G2-C or eIF2β.

The tif5-7A mutation does not impair the GTPase-activating function of eIF5 in a model in vitro assay

eIF5 stimulates hydrolysis of GTP by the TC on base pairing between Met-tRNA$_i^{Met}$ and the AUG start codon. Given that eIF5-CTD binds tightly to the β-subunit of eIF2, we considered that eIF5 GAP function could be dependent on this stable interaction with its substrate.

Hence, we investigated whether the *tif5-7A* and *tif5-12A* mutations impair eIF5 activity in an *in vitro* GAP assay. In this assay, model 48S complexes containing eIF2–[γ-^{32}P]GTP–Met-tRNA$_i^{Met}$ ternary complexes and rAUG triplets bound to 40S ribosomes are assembled from purified components, incubated with wild-type or mutant eIF5, and assayed for hydrolysis of the [γ-^{32}P]GTP bound to eIF2. For comparison purposes, we also analyzed the *ssu2-1* allele of *TIF5*, which substitutes serine for Gly62 in the N-terminus of eIF5 (Figure 6A). This mutation was isolated on the basis of reverting the Ts$^-$ phenotype conferred by the *sui1-17* mutation in eIF1 (T.F.Donahue, unpublished observations). *ssu2-1* mutant cells exhibit Slg$^-$ phenotypes at all temperatures, and grow as slowly as do *tif5-7A* mutant cells at 30°C (data not shown). As shown in Figure 6B and C, the *tif5-7A* and *ssu2-1* mutations led to similar reductions in the proportion of ribosomes present in polysomes, with a corresponding increase in the proportion of 80S monosomes.

Using the *in vitro* GAP assay described above, we found no significant differences between the activities of purified wild-type eIF5-FL and the mutant proteins eIF5-FL-12A or eIF5-FL-7A containing multiple alanine substitutions in AA-boxes 1 and 2 of the CTD, respectively (Figure 6D and E). In contrast, the *ssu2-1* mutation in the N-terminus of eIF5 led to an ~4-fold reduction in the GAP activity of purified eIF5 (T.F.Donahue, in preparation). Although this assay is non-physiological in several respects, including the absence of eIFs 1 and 3, and with an AUG triplet replacing mRNA in the 48S complex, these results suggest that the AA-boxes in eIF5-CTD are not essential for eIF5 GAP function. It is possible, however, that stable
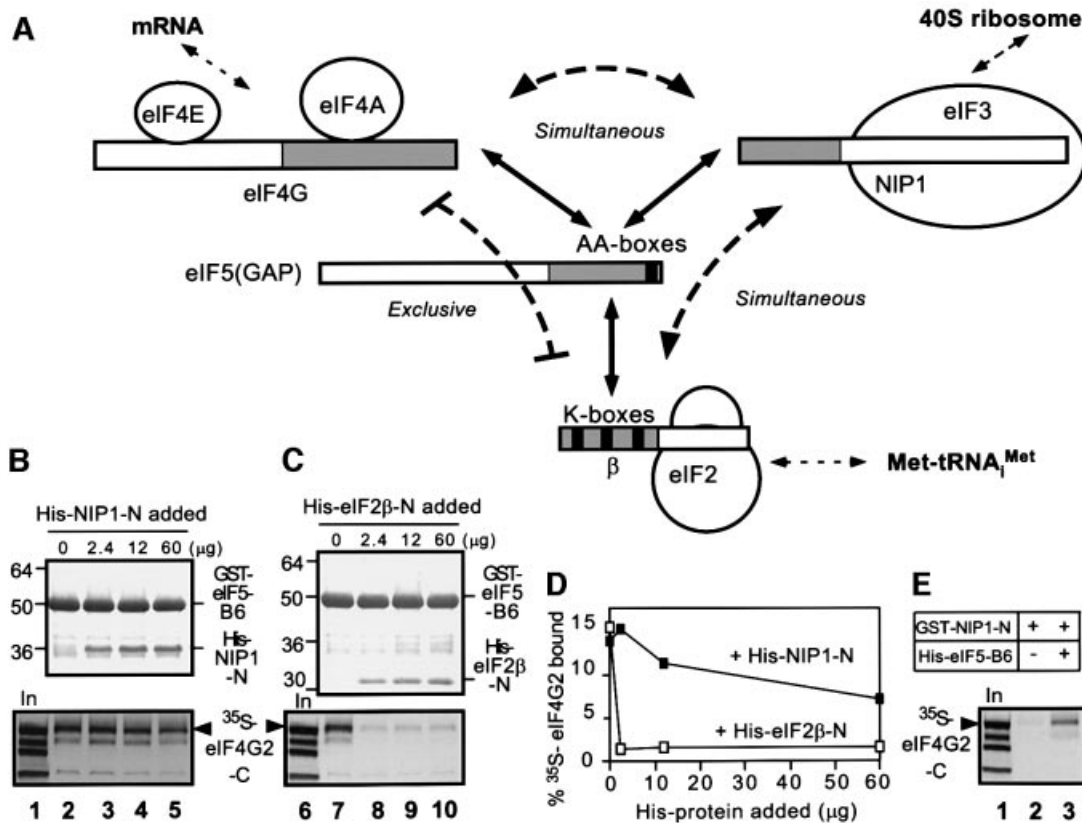
Fig. 5. eIF5 bridges interaction between eIF3 and eIF4G *in vitro*. (**A**) Schematic illustration of interactions involving eIF2β, eIF3-NIP1, eIF5 and eIF4G. Boxes denote primary structures of the proteins involved and the gray regions denote the minimal binding domains. Filled boxes denote the conserved motifs responsible for protein–protein interactions. Solid arrows indicate direct interactions, whereas curved dotted lines indicate whether the interactions occur simultaneously or exclusively. Straight dotted arrows indicate interactions with the other major components of the translation initiation complex. (**B** and **C**) Competition experiments. GST pull-down assays were conducted using 5 μg of GST–eIF5-B6 and [35S]eIF4G2-C in the presence of the indicated amounts of His-NIP-N or His-eIF2β-N. Top panels: Coomassie Blue staining following SDS–PAGE of GST–eIF5-B6 and bound His-tagged proteins recovered in the pull-down assays. Bottom panels: autoradiograms showing bound [35S]eIF4G2-C. Lanes 1 and 6, 50% input amounts of [35S]eIF4G2-C. (**D**) Graph showing the binding of [35S]eIF4G2-C plotted against the amount of each His-tagged protein added to the binding reactions. (**E**) Bridging experiments. GST pull-down assays using 5 μg of GST–NIP-N and [35S]eIF4G2-C in the presence (60 μg) or absence of His-eIF5-B6. Bound [35S]eIF4G2-C is shown in the autoradiogram. Lane 1, 50% input (In) amount of [35S]eIF4G2-C.

interactions mediated by the CTD between eIF5 and other factors in native 48S complexes promote high-level GAP activity *in vivo*. Alternatively, the concentrations of eIF5 and 48S complexes in the GAP assay may be higher than in cells, and this could compensate for impaired substrate docking with the mutant eIF5 proteins.

tif5-7A impairs association of eIF5 with 43–48S complexes and impedes a step late in the initiation pathway in vivo

To investigate the rate-limiting defect in translation initiation produced by the *tif5-7A* mutation *in vivo*, we compared the amounts of different initiation factors present on free 40S ribosomes in extracts prepared from isogenic *TIF5* and *tif5-FL-7A* strains. If the Met-tRNA$_i$^Met binding defect observed *in vitro* (Figure 1) is rate limiting *in vivo*, we would expect to find reduced amounts of eIF2 bound to free 40S ribosomes in 43–48S initiation complexes. If, however, a defect in eIF5 GAP function is rate limiting, we should observe accumulation of 48S complexes containing eIFs 1, 2 and 3 that are blocked at the step of AUG recognition prior to joining of 60S subunits. The *TIF5-FL* and *SSU2* wild-type extracts contained sizeable proportions of eIFs 2, 3 and 5 that co-

sedimented with free 40S subunits (Figure 7A and C), and also non-ribosomal pools of these factors that were present in fractions located closer to the top of the gradient. At most, only a small proportion of eIF4G co-sedimented with 40S subunits in both wild-type extracts. These results provide the first evidence that eIF5 is a stable component of 43S or 48S pre-initiation complexes *in vivo*.

It is striking that in the *tif5-7A* extract, no eIF5 co-sedimented with 40S subunits (Figure 7B), indicating that this mutation impairs stable association of eIF5 with pre-initiation complexes. Thus, eIF5-CTD is required for anchoring eIF5 to the initiation complex. In contrast, we observed increased proportions of eIF2, eIF3 and eIF1 in pre-initiation complexes in the *tif5-7A* extract versus the wild-type extract (Figure 7A and B). This was also true for eIF1 even though the total amount of eIF1 was lower in the mutant extract (Figure 7B). These results suggest that the weakened association of eIF5 with 43–48S pre-initiation complexes in *tif5-7A* cells impaired a step following recruitment of eIF3, eIF1 and TC to 40S ribosomes as the rate-limiting defect in initiation.

As opposed to the results obtained for *tif5-7A*, the *ssu2-1* mutation in the N-terminus of eIF5 did not reduce the amount of eIF5 that co-sedimented with the 43–48S
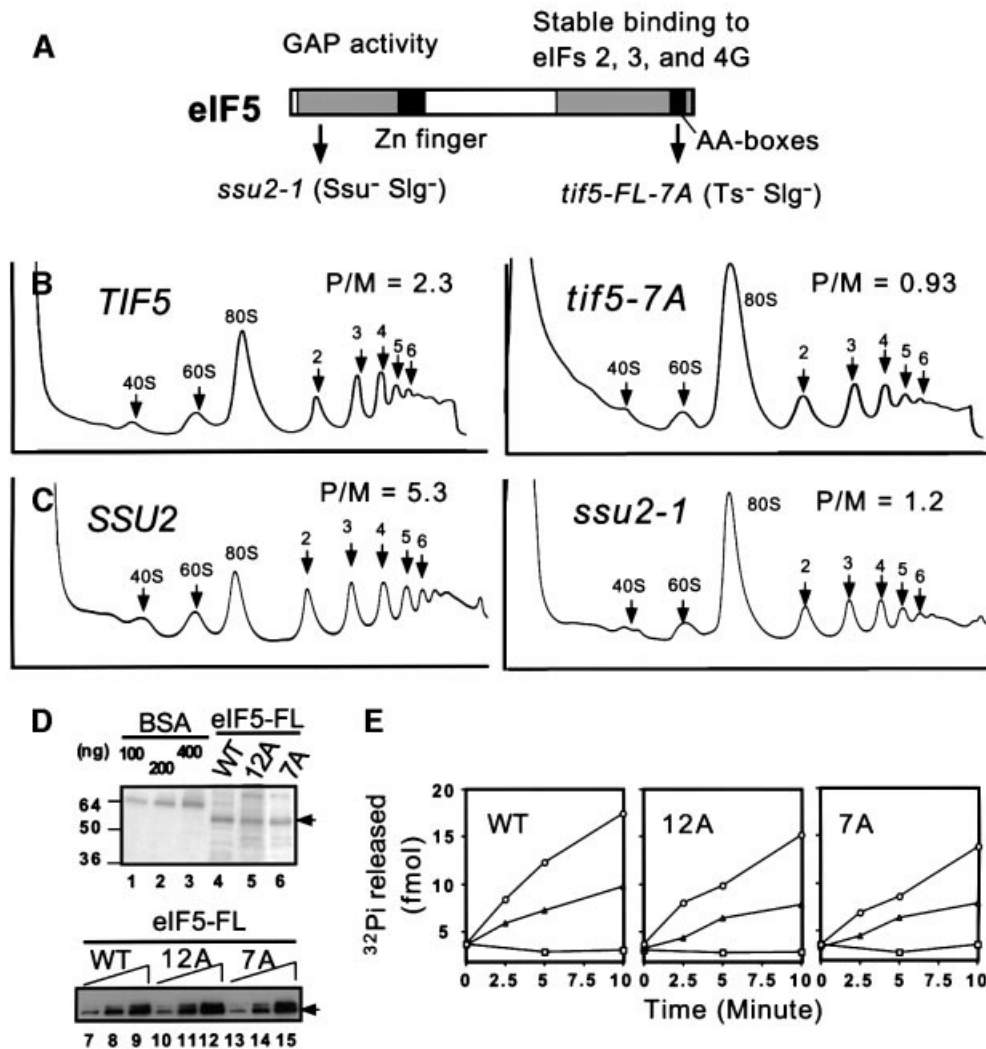
Fig. 6. Effects of eIF5 mutations in separate domains on translation initiation *in vivo* and GAP activity *in vitro*. (**A**) Primary structure of yeast eIF5 (shown by box). Gray boxes denote the regions highly conserved among its eukaryotic homologs. Filled squares denote the zinc finger motif or AA-boxes, as indicated. Arrows indicate the positions of *ssu2-1* (G62S) or *tif5-7A* mutations. The deduced roles of the N-terminal domain and CTD in GAP activity or initiation complex assembly, respectively, are indicated (see text). (**B** and **C**) Strains KAY50 (*TIF5-FL*), KAY51 (*tif5-FL-7A*) (B), or the transformants of *ssu2-1* strain JRC179–4D (α *ura3-53 his4⁻ ssu2-1*; T.F.Donahue, unpublished) carrying plasmid pKA235 (Table I) (*SSU2*) or YCplac33, the vector (*ssu2-1*) (C) were grown in YPD (B) or SC medium lacking uracil (C) at 30°C and cycloheximide was added just before harvesting the cells. WCEs were resolved on 5–45% sucrose gradients by centrifugation at 39 000 r.p.m. for 2.5 h, and the gradients were scanned continuously for A_{254}. The A_{254} profiles of the gradients are shown from top (left) to bottom (right). The positions of 40S, 60S and 80S ribosomes and polysomes of different sizes are indicated, along with the mass ratios of polysomes to 80S ribosomes (P/M). Data for (B) were taken from Asano *et al.* (2000). (**D**) Wild-type (WT) or AA-box mutant (12A or 7A) versions of eIF5-FL were purified in one step from yeast WCEs with FLAG affinity resin (see Materials and methods). Lanes 4–6 show the Coomassie Blue staining following SDS–PAGE of the eIF5-FL preparations, along with bovine serum albumin loaded as a standard (lanes 1–3). Lanes 7–15 contain 1-, 2- and 4-fold amounts of each preparation analyzed by western blotting with anti-FLAG antibodies. (**E**) eIF5 GAP assay. About 100 fmol of 48S pre-initiation complexes containing the 40S ribosome, Met-tRNA$_i$^Met, rAUG, eIF2 and [γ-^{32}P]GTP were incubated with wild-type (WT) or mutant (12A or 7A) eIF5-FL shown in (D). Aliquots were withdrawn at the indicated times and assayed for the amount of free phosphate released from the 48S complexes. Circles or triangles, 800 or 400 ng of WT or mutant eIF5-FL, respectively, were added to the reaction; squares, no eIF5 was added.

complexes. Nor did we detect any accumulation of eIFs 1, 2 or 3 in the 40–48S region (Figure 7C and D). Because the N-terminal two-thirds of eIF5 are dispensable for tight interactions with eIFs 2 and 3 *in vitro* (Asano *et al.*, 2000), these findings are consistent with the idea that only the C-terminal domain of eIF5 is required for its stable incorporation into pre-initiation complexes. [The non-ribosomal form of eIF1 was absent in the *ssu2-1* extract, as observed in the *tif5-7A* extract (Figure 7B and D). Subsequent experiments revealed that degradation of the non-ribosomal eIF1 occurred during centrifugation, as

wild-type levels of the protein were present in the unfractionated mutant extracts prepared from cyclo-heximide-treated cells (data not shown). Presumably, eIF1 dissociated from the MFC during centrifugation of the mutant extracts and was degraded by proteases.]

Our final experiments were based on the observation that the mass of free 40S ribosomes present in the 40–48S complexes relative to the amount of free 60S ribosomes was consistently lower in the *tif5-7A* mutant versus the wild-type (Figure 7A, B, E and F, top panels). Quantitation of the data from several independent experiments showed
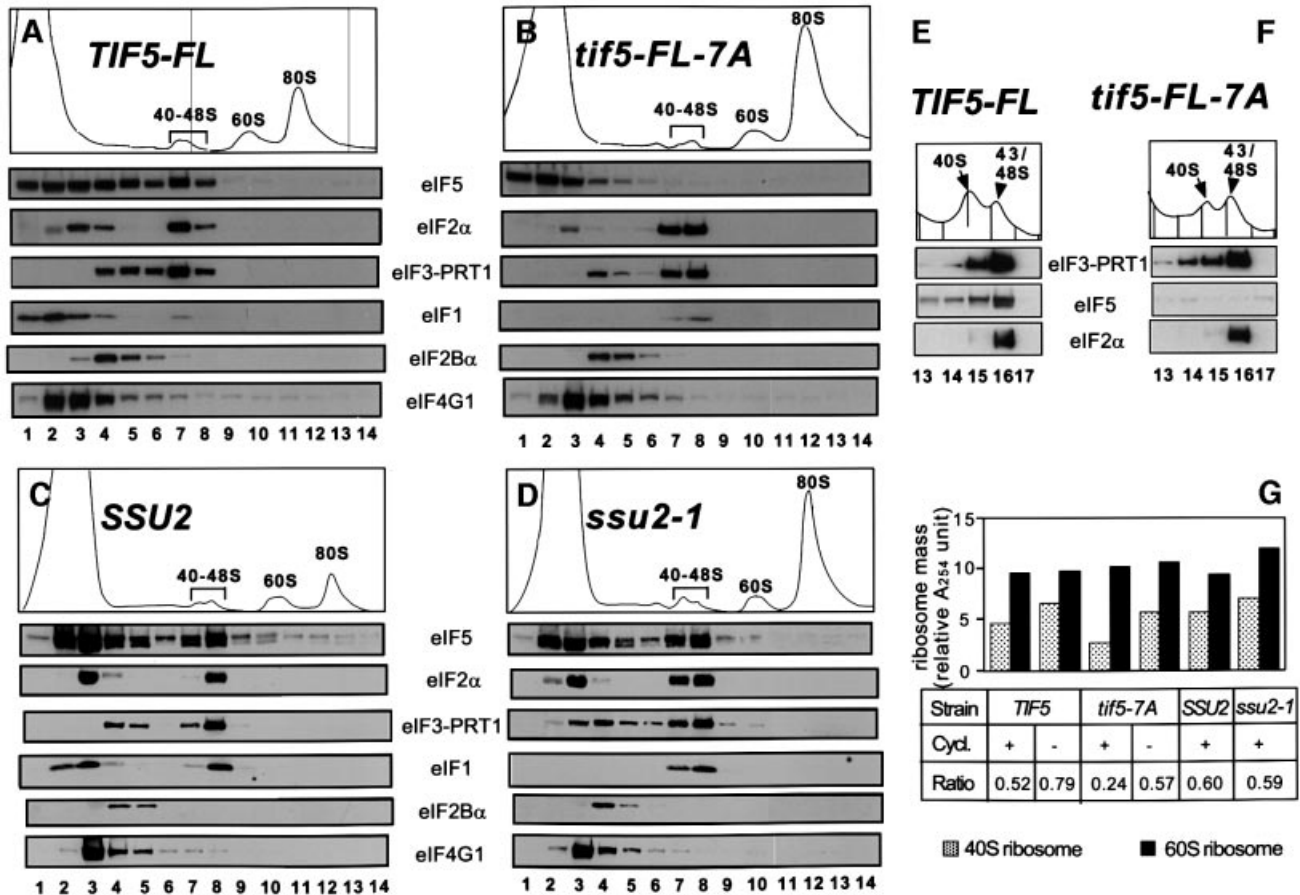
Fig. 7. The *tif5-7A* mutation impairs stable association of eIF5 with 43–48S initiation complexes and leads to accumulation of 48S complexes. (A–D) The *TIF5-FL* (**A**), *tif5-FL-7A* (**B**), *SSU2* (**C**) and *ssu2-1* (**D**) strains described in Figure 6 were grown in YPD (A and B) or SC medium lacking uracil (C and D) at 30°C, cycloheximide was added just prior to harvesting the cells and extracts were prepared in the presence of cycloheximide. Twenty A_{260} units of WCEs were fractionated on 15–40% sucrose gradients by centrifugation at 39 000 r.p.m. for 4.5 h. Top panels depict the A_{254} absorbance profiles of the gradients, and the panels below show the results of immunoblot analyses of the gradient fractions using antibodies against the factors listed next to the panels. Similar results were obtained when the strains shown in (A) and (B) were grown in SC versus YPD medium. (**E** and **F**) The same extracts analyzed in (A) and (B) were fractionated on 7.5–30% sucrose gradients by centrifugation at 41 000 r.p.m. for 5 h, and fractions 13–17 from the top of the gradient were analyzed by immunoblotting. Top panels show the A_{254} absorbance profiles for the 40–48S region of the gradient. (**G**) Histogram showing the free 40–48S and 60S subunit masses, quantitated by the area under the A_{254} profiles shown in (A)–(D) and from several independent experiments using 20 A_{260} units of extracts prepared in the presence or absence of cycloheximide. The bottom panel indicates the strains used (designated as in A–D), the presence (+) or absence (–) of cycloheximide in preparing the extracts, and the calculated 40–48S/60S ribosome mass ratio. In all these experiments, WCEs were prepared in the presence of heparin, an essential component to stabilize the 43–48S complex during sucrose gradient fractionation. The 43–48S complexes are unstable once isolated from yeast, and dissociate into the MFC and 40S subunits in the absence of heparin, as shown previously (Asano *et al.*, 2000).

that the ratio of 40S subunits in the 40–48S fractions to free 60S subunits was 0.24 ± 0.019 in the *tif5-7A* mutant compared with 0.52 ± 0.056 in the wild type (Figure 7G). Because the proportions of non-ribosomal eIF2 and eIF3 present near the top of the gradient were also reduced in the *tif5-7A* mutant (Figure 7A and B, lanes 2–5), it seemed likely that 40S ribosomes were sequestered in the polysomes in the form of 48S complexes containing the TC. If this interpretation is correct, then 40S ribosomes lacking bound eIF2 should be depleted from the 40–48S region in the *tif5-7A* extract. To test this prediction, we used centrifugation conditions that produced a greater separation of ribosomal species in the 40–48S region and probed the fractions for eIFs 2, 3 and 5. As shown in Figure 7E, there were two peaks evident in the 40–48S region of the wild-type extract, of which the smaller lacked eIF2 and had relatively low levels of eIFs 3 and 5. This 40S

peak lacking eIF2 was specifically depleted in the *tif5-7A* mutant, consistent with a depletion of free 40S subunits lacking the TC (Figure 7F). As expected, eIF5 was absent from the 43–48S ribosomes in the mutant (Figure 7F).

To test our interpretation that the free 40S subunits absent in the *tif5-7A* mutant are sequestered in polysomes as 48S complexes, we asked whether disruption of the polysomes would restore the amount of free 40S ribosomes in the *tif5-7A* extract to the wild-type level. When the extracts were prepared in the absence of cycloheximide, most of the polysomes were lost, with concomitant accumulation of vacant 80S couples, as a consequence of polysome run-off (data not shown) (Foiani *et al.*, 1991). The amount of free 60S subunits was not altered by the polysome run-off (Figure 7G), suggesting that most of the 80S ribosomes were released from polysomes without being dissociated into free subunits.

In accordance with our prediction, the amount of 40S ribosomes in the 40–48S fractions increased significantly in the mutant following polysome run-off, approaching the value observed in the wild-type strain under the same conditions (Figure 7G). Furthermore, the non-ribosomal pool of eIF2, which is depleted in the mutant (Figure 7B), increased to the wild-type level in the absence of cycloheximide (data not shown). These findings support the idea that a greater proportion of 40S ribosomes are distributed throughout the polysome fractions, most likely as 48S complexes, in the *tif5-7A* mutant versus the wild-type strain.

In contrast, the *ssu2-1* mutation did not lead to a low level of free 40S subunits (Figure 7C and D), and the 40–48S:60S free subunit ratios for the isogenic *ssu2-1* and *SSU2* strains were virtually identical (Figure 7G). These results are in accordance with the fact that eIF2 and eIF3 did not accumulate in the 40–48S fractions in the *ssu2-1* mutant (Figure 7C and D). Hence, it appears that a catalytic defect in eIF5 GAP activity produced by *ssu2-1* does not lead to accumulation of 48S complexes stalled at the AUG start codon. Presumably, these complexes decay quickly into free eIFs and 40S subunits, rather than accumulating in the polysome fractions. The fact that 48S complexes lacking eIF5 accumulated in the *tif5-7A* mutant may have important implications concerning the steps in AUG recognition and GTP hydrolysis that are impaired when eIF5 is not stably anchored to the pre-initiation complex.

Discussion

Role of eIF5-CTD in stabilizing 43S and 48S complexes

eIF3 can bind to 40S ribosomes and is required for recruitment of the TC in cell extracts (Trachsel *et al.*, 1977; Benne and Hershey, 1978; Phan *et al.*, 1998), but the molecular interactions involved in this activity are poorly understood. The *tif5-7A* mutation altering eIF5-CTD is known to destabilize formation of an MFC containing eIFs 1, 2, 3 and 5, and tRNA$_i^{Met}$ (Asano *et al.*, 2000) (box 1 in Figure 8). We found that binding of exogenous Met-tRNA$_i^{Met}$ to the 40S ribosome was diminished in an extract from the *tif5-7A* mutant, and this defect was complemented by addition of purified eIF5 (Figure 1A and B). These results suggest that, by linking eIF2 and eIF3 in the MFC, eIF5-CTD stimulates binding of TC to the 40S subunit to form the 43S pre-initiation complex.

Binding of exogenous mRNA to the 40S ribosome was also defective in the *tif5-7A* extract, and could be rescued with purified eIF5 (Figure 1C–E). While this mRNA binding defect may result indirectly from reduced TC binding, it led us to investigate whether eIF5-CTD interacts with eIF4G, an adaptor subunit of the eIF4F complex that promotes mRNA binding to 40S ribosomes. Using purified proteins, we showed that eIF4G binds directly to eIF5-CTD, in a manner stimulated by the AA-boxes (Figures 3 and 4), and this interaction can occur simultaneously with association between eIF5-CTD and eIF3-NIP1 (Figure 5B and E). It is thought that direct interaction between eIF3 and eIF4G promotes mRNA binding to ribosomes in mammalian cells (Hentze, 1997; Sachs *et al.*, 1997). The ability of eIF5-CTD to interact simultaneously with eIF3-NIP1 and eIF4G may help to stabilize the eIF3–eIF4G interaction and promote mRNA binding. Supporting this idea, co-immunoprecipitation of native eIF4G and eIF3 was reduced by the *tif5-7A* mutation in the eIF5-CTD (Figure 2).

The eIF5–eIF4G interaction was of lower affinity, and mutually exclusive with the eIF5–eIF2β interaction (Figure 5C and D), suggesting that the two interactions occur at different steps in the initiation pathway. The eIF2β–eIF5-CTD association occurs in the MFC free of the ribosome (Asano *et al.*, 2000), and helps to recruit eIF5 to the 43S complex in proper juxtaposition with TC, eIF1 and eIF3. This interaction may give way to eIF4G–eIF5-CTD interaction in the 48S complex to promote mRNA binding or facilitate scanning (Figure 8). Because the K-boxes in eIF2 mediate mRNA binding by eIF2 (Laurino *et al.*, 1999), the mRNA–eIF2β interaction in the 48S complex may displace eIF5 from the K-boxes, allowing the lower affinity eIF5–eIF4G interaction to proceed (box 2 in Figure 8).

Distinct requirements for the C- and N-terminal domains of eIF5 in initiation complex formation and GAP activity

The *tif5-7A* mutation reduced Met-tRNA$_i^{Met}$ binding to 40S ribosomes *in vitro* (Figure 1), suggesting that eIF5-CTD enhances the rate of TC binding to 40S subunits, or the stability of the 43S complex in cell extracts. Ostensibly at odds with this finding, we observed accumulation of eIF2 on free 40S subunits and a reduction in the non-ribosomal pool of this factor in *tif5-7A* cells (Figure 7A and B). Moreover, we deduced that polysome-associated 48S complexes accumulated in *tif5-7A* cells, accounting for the observed depletion of free 40S subunits lacking bound eIF2 (Figure 7B, F and G). Thus, it appears that conversion of 48S to 80S initiation complexes is the rate-limiting defect responsible for the reduced rate of translation initiation in this mutant. We presume that the rate of 43S complex formation is also reduced in *tif5-7A* cells, as seen *in vitro* (Figure 1), but, because the defect in 48S to 80S conversion is more severe, we observed accumulation of 48S complexes. Importantly, eIF5 was lost from 43–48S complexes in *tif5-7A* cells, showing that eIF5-CTD is crucial for stable incorporation of eIF5 into the initiation complex (Figure 7A and B). Hence, the absence of eIF5 from 48S complexes impedes their conversion to 80S complexes. In principle, this could occur by a reduction in the rate of scanning from the 5′ cap, reduced activation of GTP hydrolysis on AUG recognition or impaired 60S subunit joining following GTP hydrolysis.

We observed little or no effect of the *tif5-7A* or *tif5-12A* mutations on the ability of purified eIF5 to stimulate GTP hydrolysis by model 48S complexes containing the TC and AUG triplets bound to 40S subunits (Figure 6D and E). Although these assay conditions are non-physiological in several respects, our data suggest that the AA-boxes in eIF5-CTD are not required for the catalytic activity of eIF5. In the same assay, the *ssu2-1* mutation in the N-terminus of eIF5 (G62S) leads to a substantial reduction in GAP activity. Consistently, *ssu2-1* reduced the rate of translation initiation (Figure 6C) but did not diminish the amount of eIF5 associated with the 43–48S complexes *in vivo* (Figure 7D). Accordingly, we propose that *ssu2-1*
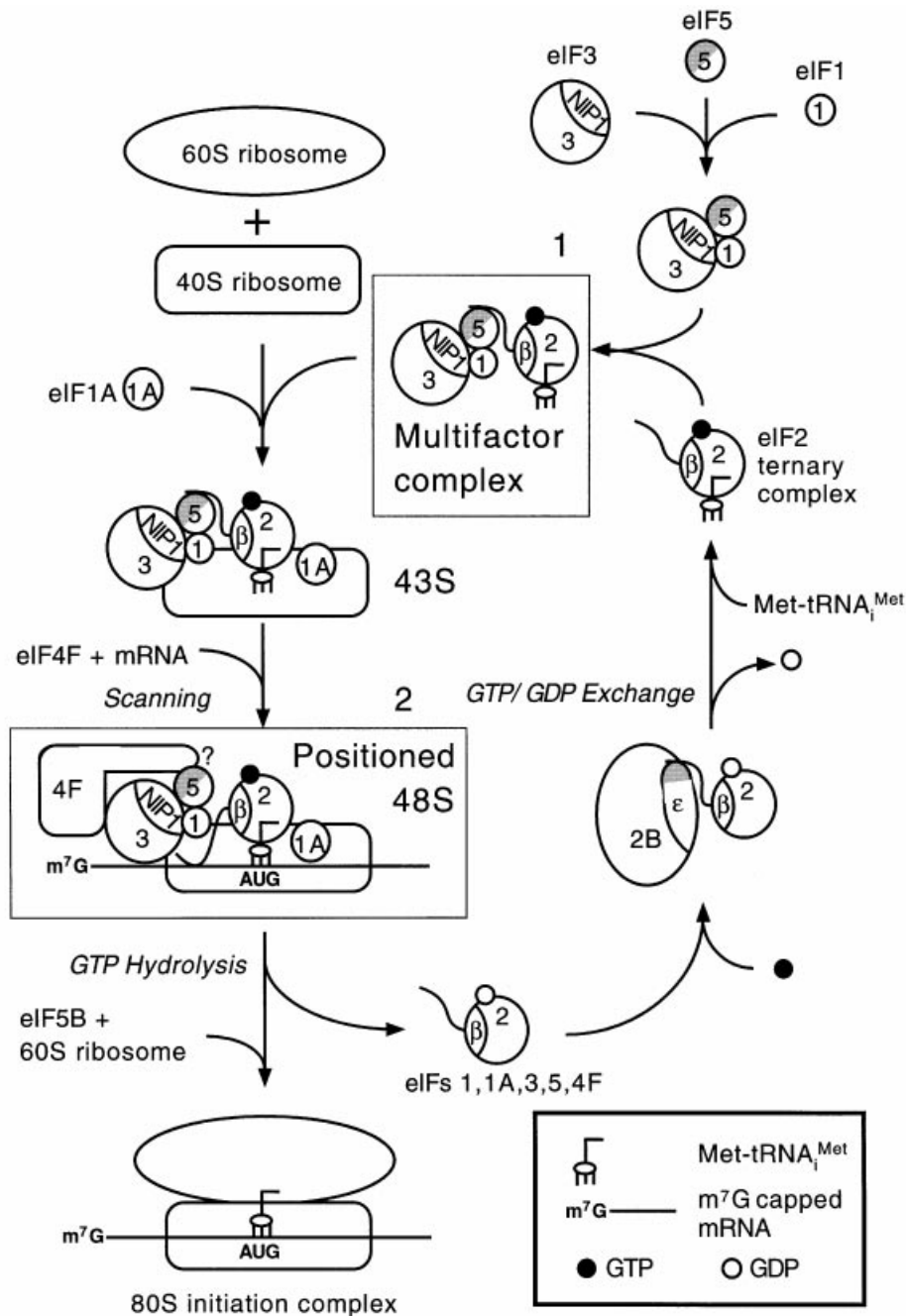
Fig. 8. Hypothetical model for the role of eIF5-CTD in assembling the translation initiation complex in *S.cerevisiae*. The CTD (gray half circle) of eIF5 (5), containing the conserved AA-boxes, bridges interaction between eIF3-NIP1 (3) and eIF2β (2) and mediates formation of the MFC, also containing Met-tRNA$_i^{Met}$ and eIF1 (box 1) (Asano *et al.*, 2000). The wavy line on eIF2β represents the K-box domain, the binding site for eIF5-CTD. As the MFC occurs free of the ribosomes, it could carry out the recruitment of TC, eIFs 1, 3 and 5 in a single step, to form the 43S complex. The eIF1A (1A) may bind directly to the 40S ribosome (Hershey and Merrick, 2000). Capped poly(A) mRNA bound to eIF4F is recruited to the 43S complex by interactions between eIF3 and the eIF4G subunit of eIF4F. The eIF2β–eIF5 interaction in the MFC may be replaced by eIF4G–eIF5 interaction in the 48S complex, possibly when eIF2β interacts with mRNA. The eIF4G–eIF5 and eIF2β–mRNA interactions help stabilize the 48S complex. The 48S complex scans to the AUG start codon. Base pairing between AUG and Met-tRNA$_i^{Met}$ triggers hydrolysis of GTP bound to eIF2, dependent on the eIF5 N-terminal domain (white half circle), followed by ejection of eIF2-GDP and other eIFs. Joining of the 60S subunit is stimulated by eIF5B. The GDP bound to eIF2 is subsequently replaced with GTP by the guanine nucleotide exchange factor eIF2B (2B). This last interaction is mediated at least partly by a second AA-box-containing motif (shown as gray shading) in the catalytic (ε) subunit of eIF2B (Asano *et al.*, 1999). Our results indicate that formation of the MFC is required for efficient binding of Met-tRNA$_i^{Met}$ and mRNA to 40S ribosomes. It is also required for stable incorporation of eIF5 into 48S complexes and conversion of 48S to 80S complexes. The latter appears to be the rate-limiting defect in initiation produced by the *tif5-7A* mutation in eIF5-CTD, which destabilizes the MFC.

impairs the GAP activity of eIF5, lodged in the N-terminus of the protein, but not its interactions with other eIFs in 43–48S initiation complexes. In contrast, *tif5-7A* would leave the catalytic activity of eIF5 largely intact while eliminating this factor as an integral component of 48S complexes. This model is consistent with the previous

Table I. Plasmids employed in this study

Plasmid	Description[a]	Product	Source
pGEX vectors	expression vectors for GST fusions	GST	Pharmacia
pAS466	full-length *TIF4631* ORF in pGEX	GST–eIF4G1	Tarun and Sachs (1996)
pAS467	full-length *TIF4632* ORF in pGEX	GST–eIF4G2	Tarun and Sachs (1996)
pGEX-TIF5	full-length *TIF5* ORF in pGEX	GST–eIF5	Phan *et al.* (1998)
pGEX-B6	*TIF5* ORF (241–405) in pGEX	GST–eIF5-B6	Asano *et al.* (1999)
pGEX-B6-12A	pGEX-B6 carrying *tif5-12A*	GST–eIF5-B6-12A	this study
pGEX-B6-7A	pGEX-B6 carrying *tif5-7A*	GST–eIF5-B6-7A	this study
pGEX-NIP1-N	*NIP1* ORF (1–156) in pGEX	GST–NIP1-N	Asano *et al.* (2000)
pT7-7	expression vector with T7 promoter		Tabor and Richardson (1987)
pT7-4G2ΔN	*TIF4632* ORF (1–513) in pT7-7	eIF4G2-N	this study
pT7-4G2ΔS	*TIF4632* ORF (439–914) in pT7-7	eIF4G2-C	this study
pT7-TIF5	full-length *TIF5-FL* in pT7-7	eIF5-FL	Asano *et al.* (2000)
pT7-TIF5-7A	pT7-TIF5 carrying tif5-7A	eIF5-FL-7A	Asano *et al.* (2000)
pET15b	expression vector for polyhistidine-tagged proteins		Novagen
pHis-NIP1-N	*NIP1* ORF (1–156) in pET15b	His-NIP1-N	Asano *et al.* (2000)
pHis-TIF5-B6	*TIF5* ORF (241–405) in pET15b	His-eIF5-B6	Asano *et al.* (2000)
pHis-SUI3ΔS	*SUI3* ORF (1–140) in pET15b	His-eIF2β-N	this study
pKA235	CEN plasmid carrying *TIF5 URA3*		Asano *et al.* (1999)

[a]Numbers in parentheses indicate amino acid positions at the termini of the relevant protein segment.

finding that the Sui⁻ mutation in eIF5 altering Gly31 to arginine increased GAP activity *in vitro* by ~2-fold (Huang *et al.*, 1997).

Even if the CTD is not required for eIF5 catalytic function, the loss of eIF5 from 48S pre-initiation complexes in the *tif5-7A* mutant might reduce the rate of GTP hydrolysis *in vivo* by decreasing the concentration of eIF5 in the vicinity of 48S complexes paired with start codons. In principle, a defect in this 'substrate docking' function of the CTD should have been detected in our GAP assays, and indeed Das and Maitra (2000) reported that alteration of acidic residues in the AA-boxes of rat eIF5 reduced GAP activity *in vitro* with concomitant decreases in binding to recombinant eIF2β. These workers used a model 48S complex composed of mammalian components, whereas ours contained the corresponding yeast components. Perhaps the catalytic step, rather than substrate binding, is rate limiting in GAP assays using model 48S complexes from yeast.

Another way to explain the defect in 48S to 80S conversion in *tif5-7A* mutants is to propose that eIF5 must be positioned precisely in native 48S complexes in order to trigger GTP hydrolysis with maximum efficiency. It is known that eIF5 can not stimulate GTP hydrolysis by the TC unless both factors are bound to the 40S subunit and the Met-tRNAᵢ^Met is base paired with AUG (Chakrabarti and Maitra, 1991). Hence, GTP hydrolysis may require conformational changes on recognition of the start codon that depend on proper juxtaposition of eIF5 with other components of the MFC or with eIF4G. This hypothetical function of eIF5-CTD could be bypassed in model 48S complexes containing only the TC, or at the non-physiological Mg²⁺ concentrations used for *in vitro* GAP assays.

The fact that 48S complexes accumulated in *tif5-7A* but not in *ssu2-1* cells (Figure 7B, D and G) suggests that different steps in the maturation of 48S complexes are disrupted by these mutations. Perhaps impaired interaction of eIF5 with eIF4G in the *tif5-7A* mutant impedes the rate of scanning, so that base pairing between the Met-tRNAᵢ^Met and AUG codon is delayed. Considering

that eIF1 also interacts with eIF5-CTD (Asano *et al.*, 2000) and has been implicated in AUG recognition (Pestova *et al.*, 1998; Donahue, 2000), *tif5-7A* may impair the function of eIF1 in AUG recognition during scanning. The reduced rate of scanning would account for the accumulation of 48S complexes observed in *tif5-7A* cells. If *ssu2-1* impairs only the GAP activity of eIF5, then 48S complexes should be stalled at the AUG start codon in this mutant. The fact that 48S complexes did not accumulate in *ssu2-1* cells suggests that 48S complexes positioned at an AUG will decay to free 40S subunits if GTP hydrolysis does not occur in a prescribed period of time.

Materials and methods

Materials
Plasmids employed in this study are listed in Table I. Details of their construction are available upon request. His-eIF2β-N, His-NIP1-N and His-eIF5-B6 were expressed in *Escherichia coli* strain BL21(DE3) from the appropriate pET15b derivatives (Table I), purified with Ni²⁺ affinity resin (Novagen) as recommended by the manufacturer and dialyzed against the GST pull-down buffer (Asano *et al.*, 1998) without milk. To purify eIF5-FL proteins from yeast, 10 mg of WCEs were prepared in buffer A (Asano *et al.*, 1999) from KAY39, KAY40 and KAY58, encoding wild-type, *tif5-7A* and *tif5-12A* forms of eIF5 in high copy (Asano *et al.*, 1999), and incubated with 100 μl of anti-FLAG affinity resin (Sigma) at 4°C for 2 h. After washing with buffer A, beads were eluted with 400 ng/μl FLAG peptide (Sigma) in 200 μl of buffer A. eIF5-FL or its *tif5-7A* derivative were purified similarly from BL21(DE3) transformants carrying pT7-TIF5 or pT7-TIF5-7A grown in the presence of isopropyl-β-D-thiogalactopyranoside (IPTG). Yeast eIF2 (Pavitt *et al.*, 1998), [³H]Met-tRNAᵢ^Met (Phan *et al.*, 1998), uncapped [³²P]poly(A) *MFA2* mRNA (Tarun and Sachs, 1995) and 40S ribosomes (Huang *et al.*, 1997) were prepared as described previously.

Biochemical assays
Immunoprecipitations with antibodies against the HA epitope were conducted as described (Asano *et al.*, 1998, 1999). Rabbit polyclonal antibodies used for immunoblot analysis are listed in Asano *et al.* (1999), except those against eIF1 (Yoon and Donahue, 1992), eIF5 (Huang *et al.*, 1997), eIF2Bα (Cigan *et al.*, 1991), eIF4G1 (Wells *et al.*, 1998) and eIF4E (Lang *et al.*, 1994). GST pull-down assays were conducted as described previously (Asano *et al.*, 1999, 2000). For RNase treatment in pull-down assays, GST–eIF4G–eIF5-FL complexes attached to glutathione–Sepharose were incubated with 20 μg of RNase A (Sigma) at 26°C for 5 min or 120 U of micrococcal nuclease (USB) at 4°C for

30 min and washed extensively, prior to separation by SDS–PAGE (Tarun and Sachs, 1996; Winstall *et al.*, 2000).

Binding of [³H]Met-tRNAᵢMet and [³²P]poly(A) *MFA2* mRNA to 40S ribosomes was assayed in cell extracts as described previously (Phan *et al.*, 1998). A 20 µl aliquot of the extracts was pre-incubated with 6 µl of buffer A (Asano *et al.*, 1999) containing the indicated amounts of eIF5 on ice for 5 min, and then incubated with 26 µl of 2× buffer (Phan *et al.*, 1998) containing 2.4 mM GMPPNP, [³H]Met-tRNAᵢMet (0.77 µCi, 84 Ci/mmol) and [³²P]poly(A) *MFA2* mRNA (2.0 µCi, 5.6 Ci/mmol) for 20 min at 26°C. After adding 6 µl of 3% formaldehyde, the sample was loaded on a 7.5–30% sucrose gradient prepared in buffer (20 mM Tris–HCl pH 7.5, 100 mM KCl, 1 mM MgCl₂) and centrifuged at 41 000 r.p.m. for 5 h at 4°C in a Beckman SW41 rotor. The gradient was separated into 20 fractions of 0.6 ml with an ISCO gradient fractionater while scanning continuously at 254 nm, and 0.2 ml of each fraction was diluted in 1 ml of water and mixed with 10 ml of Ecolite™ cocktail for liquid scintillation counting of ³H and ³²P radioactivity. A model 48S complex containing the 40S ribosome, rAUG and eIF2–[γ-³²P]GTP–Met-tRNAᵢMet ternary complex was prepared and employed as substrate in GAP assays of purified eIF5 as described previously (Huang *et al.*, 1997).

Polysome analysis was conducted as previously described (Asano *et al.*, 2000).

Acknowledgements

We are indebted to Alan Sachs for his gifts of materials and to Han Huang for advice on the GAP assay. We thank Thanuja Krishnamoorthy for purified yeast eIF2, Salvador Tarun for advice on eIF4G binding experiments, Gota Kawai for discussion, Tom Dever for comments on the manuscript, and members of the Hinnebusch and Dever laboratories for advice. A.S. was supported by an Endocrine Fellowship from the Diabetes Branch, NIDDK, NIH.

References

Asano,K., Phan,L., Anderson,J. and Hinnebusch,A.G. (1998) Complex formation by all five homologues of mammalian translation initiation factor 3 subunits from yeast *Saccharomyces cerevisiae*. *J. Biol. Chem.*, **273**, 18573–18585.

Asano,K., Krishnamoorthy,T., Phan,L., Pavitt,G.D. and Hinnebusch, A.G. (1999) Conserved bipartite motifs in yeast eIF5 and eIF2Bε, GTPase-activating and GDP–GTP exchange factors in translation initiation, mediate binding to their common substrate eIF2. *EMBO J.*, **18**, 1673–1688.

Asano,K., Clayton,J., Shalev,A. and Hinnebusch,A.G. (2000) A multifactor complex of eukaryotic initiation factors eIF1, eIF2, eIF3, eIF5 and initiator tRNAMet is an important translation initiation intermediate *in vivo*. *Genes Dev.*, **14**, 2534–2546.

Benne,R. and Hershey,J.W.B. (1978) The mechanism of action of protein synthesis initiation factors from rabbit reticulocytes. *J. Biol. Chem.*, **253**, 3078–3087.

Chakrabarti,A. and Maitra,U. (1991) Function of eukaryotic initiation factor 5 in the formation of an 80S ribosomal polypeptide chain initiation complex. *J. Biol. Chem.*, **266**, 14039–14045.

Cigan,A.M., Foiani,M., Hannig,E.M. and Hinnebusch,A.G. (1991) Complex formation by positive and negative translational regulators of *GCN4*. *Mol. Cell. Biol.*, **11**, 3217–3228.

Das,S. and Maitra,U. (2000) Mutational analysis of mammalian translation initiation factor 5 (eIF5): role of interaction between the β subunit of eIF2 and eIF5 in eIF5 function *in vitro* and *in vivo*. *Mol. Cell. Biol.*, **20**, 3942–3950.

Das,S., Maiti,T., Das,K. and Maitra,U. (1997) Specific interaction of eukaryotic translation initiation factor 5 (eIF5) with the β-subunit of eIF2. *J. Biol. Chem.*, **272**, 31712–31718.

Donahue,T. (2000) Genetic approaches to translation initiation in *Saccharomyces cerevisiae*. In Sonenberg,N., Hershey,J.W.B. and Mathews,M.B. (eds), *Translational Control of Gene Expression*. Cold Spring Harbor Laboratory Press, Cold Spring Harbor, NY, pp. 487–502.

Foiani,M., Cigan,A.M., Paddon,C.J., Harashima,S. and Hinnebusch,A.G. (1991) GCD2, a translational repressor of the *GCN4* gene, has a general function in the initiation of protein synthesis in *Saccharomyces cerevisiae*. *Mol. Cell. Biol.*, **11**, 3203–3216.

Hentze,M.W. (1997) eIF4G: a multipurpose ribosome adapter. *Science*, **275**, 500–501.

Hershey,J.W.B. and Merrick,W.C. (2000) Pathway and mechanism of initiation of protein synthesis. In Sonenberg,N., Hershey,J.W.B. and Mathews,M.B. (eds), *Translational Control of Gene Expression*. Cold Spring Harbor Laboratory Press, Cold Spring Harbor, NY, pp. 33–88.

Hinnebusch,A.G. (2000) Mechanism and regulation of initiator methionyl-tRNA binding to ribosomes. In Sonenberg,N., Hershey, J.W.B. and Mathews,M.B. (eds), *Translational Control of Gene Expression*. Cold Spring Harbor Laboratory Press, Cold Spring Harbor, NY, pp. 185–243.

Huang,H., Yoon,H., Hannig,E.M. and Donahue,T.F. (1997) GTP hydrolysis controls stringent selection of the AUG start codon during translation initiation in *Saccharomyces cerevisiae*. *Genes Dev.*, **11**, 2396–2413.

Lang,V., Zanchin,N.I., Lunsdorf,H., Tuite,M. and McCarthy,J.E. (1994) Initiation factor eIF-4E of *Saccharomyces cerevisiae*. Distribution within the cell, binding to mRNA and consequences of its overproduction. *J. Biol. Chem.*, **269**, 6117–6123.

Laurino,J.P., Thompson,G.M., Pacheco,E. and Castilho,B.A. (1999) The β subunit of eukaryotic translation initiation factor 2 binds mRNA through the lysine repeats and a region comprising the C₂–C₂ motif. *Mol. Cell. Biol.*, **19**, 173–181.

Neff,C.L. and Sachs,A.B. (1999) Eukaryotic translation initiation factors eIF4G and eIF4A from *Saccharomyces cerevisiae* physically and functionally interact. *Mol. Cell. Biol.*, **19**, 5557–5564.

Pavitt,G.D., Ramaiah,K.V.A., Kimball,S.R. and Hinnebusch,A.G. (1998) eIF2 independently binds two distinct eIF2B subcomplexes that catalyze and regulate guanine-nucleotide exchange. *Genes Dev.*, **12**, 514–526.

Pestova,T.V., Borukhov,S.I. and Hellen,C.U.T. (1998) Eukaryotic ribosomes require initiation factors 1 and 1A to locate initiation codons. *Nature*, **394**, 854–859.

Phan,L., Zhang,X., Asano,K., Anderson,J., Vornlocher,H.P., Greenberg, J.R., Qin,J. and Hinnebusch,A.G. (1998) Identification of a translation initiation factor 3 (eIF3) core complex, conserved in yeast and mammals, that interacts with eIF5. *Mol. Cell. Biol.*, **18**, 4935–4946.

Sachs,A.B., Sarnow,P. and Hentze,M.W. (1997) Starting at the beginning, middle and end: translation initiation in eukaryotes. *Cell*, **89**, 831–838.

Tabor,S. and Richardson,C.C. (1987) DNA sequence analysis with a modified bacteriophage T7 DNA polymerase. *Proc. Natl Acad. Sci. USA*, **84**, 4767–4771.

Tarun,S.Z. and Sachs,A.B. (1995) A common function for mRNA 5′ and 3′ ends in translation initiation in yeast. *Genes Dev.*, **9**, 2997–3007.

Tarun,S.Z. and Sachs,A.B. (1996) Association of the yeast poly(A) tail binding protein with translation initiation factor eIF-4G. *EMBO J.*, **15**, 7168–7177.

Trachsel,H., Erni,B., Schreier,M.H. and Staehelin,T. (1977) Initiation of mammalian protein synthesis: the assembly of the initiation complex with purified initiation factors. *J. Mol. Biol.*, **116**, 755–767.

Wells,S.E., Hillner,P.E., Vale,R.D. and Sachs,A.B. (1998) Circularization of mRNA by eukaryotic translation initiation factors. *Mol. Cell*, **2**, 135–140.

Winstall,E., Sadowski,M., Kuhn,U., Wahle,E. and Sachs,A.B. (2000) The *Saccharomyces cerevisiae* RNA-binding protein Rbp29 functions in cytoplasmic mRNA metabolism. *J. Biol. Chem.*, **275**, 21817–21826.

Yoon,H.J. and Donahue,T.F. (1992) The *sui1* suppressor locus in *Saccharomyces cerevisiae* encodes a translation factor that functions during tRNAᵢMet recognition of the start codon. *Mol. Cell. Biol.*, **12**, 248–260.